ACS OMEGA

http://pubs.acs.org/journal/acsodf

Article

Gold Nanoparticles Generated Using the Nanosecond Laser Treatment of Multilayer Films and Their Use for SERS Applications

Evaldas Stankevičius,* Ilja Ignatjev, Vita Petrikaitė, Algirdas Selskis, and Gediminas Niaura

Cite This: *ACS Omega* 2021, 6, 33889−33898

Read Online

ACCESS | Metrics & More | Article Recommendations | Supporting Information

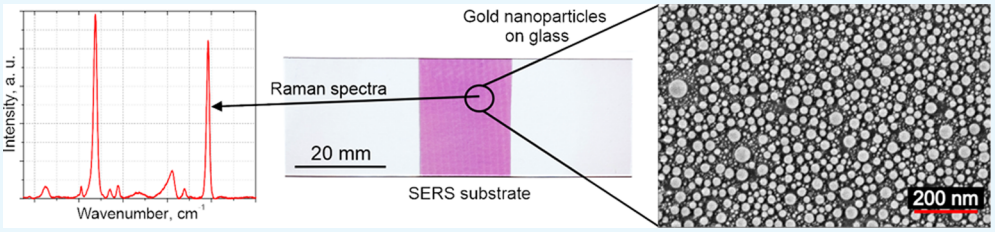

ABSTRACT: Surface-enhanced Raman spectroscopy (SERS) substrates fabricated using a repeated laser treatment of thin gold films are demonstrated. The presented SERS substrates consist of the gold nanoparticles, whose density and size depend on the used film thickness and number of treated films. The larger number of the treated gold film layers increases the amount of larger nanoparticles (size >20 nm). However, a large number of small nanoparticles (5−20 nm) in all cases is also observed. The manufactured SERS substrates exhibit a high enhancement factor, which is in the range of 10^6. The enhancement factor can be increased by adding an additional Au coating on the top of nanoparticles generated from a single gold layer. The demonstrated laser-based fabrication approach of large-scale SERS substrates is simple, reliable, without the use of chemicals for the reduction and stabilization of nanoparticles, and cost-effective.

1. INTRODUCTION

Since the discovery of surface-enhanced Raman spectroscopy (SERS) in 1974,[1] a lot of studies related to the enhancement of Raman signals have been implemented due to the SERS ability to analyze biomolecules and chemical molecules with ultra-high sensitivity.[2,3] The increase in the Raman signal mainly appears due to the electromagnetic enhancement, which is mostly determined by the localized surface plasmon resonance (LSPR). As the Raman shift is small compared to the LSPR bandwidth,[4] the field of both the incident and emitted light is enhanced. It leads to the total electric field enhancement by four orders of magnitude (E^4). The match of the excitation wavelength and the LSPR can significantly increase the enhancement factor (EF) of the SERS substrate due to the enhancement of the local electromagnetic field at the metal−dielectric interfaces summoned by the local charge oscillations at the structure edges.[5−8] The EF is one of the essential parameters of SERS substrates, which shows by how many times the enhancement of the Raman signal by the substrate is higher than that of the molecule far from the surface.[9−11] This parameter strongly depends on the metal nature, size, gaps, and shape of the nanostructures.

Each fabrication method of the SERS substrate is specific and has its own pros and cons. SERS substrates can be fabricated using electron-beam lithography,[12−14] focused ion beam,[15,16] laser treatment of thin gold films,[17−19] nanosphere lithography,[20−22] nanowires decorated with nanoparticles,[23−25] nanorods from oblique angle deposition,[26−29] nanoclusters from colloidal aggregation,[30,31] rough thin films from chemical roughening,[32] electrochemical roughening,[33,34] metallic film annealing,[35,36] and nanoimprint lithography.[37,38] It should be noted that the common problem in the case of substrates prepared by the chemical approach is the contamination of surfaces by molecules used for the reduction or stabilization of nanoparticles.[39] The adsorbed impurities present compete for adsorption sites with target compounds and exhibit SERS bands, obscuring the spectrum of molecules under investigation and therefore significantly reducing the sensing ability of plasmonic substrates. Thus, though the SERS substrates can be fabricated using various methods, there is still a need to develop SERS substrates with high EFs, excellent reliability, the absence of adsorbed impurities, and good scalability at low cost.

Here, the simple fabrication method of SERS substrates using a repeated process of a thin gold coating deposition and laser treatment of films is demonstrated. The presented approach does not use complicated procedures such as etching

Received: September 17, 2021
Accepted: November 8, 2021
Published: November 22, 2021

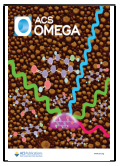

https://doi.org/10.1021/acsomega.1c05165
ACS Omega 2021, 6, 33889−33898

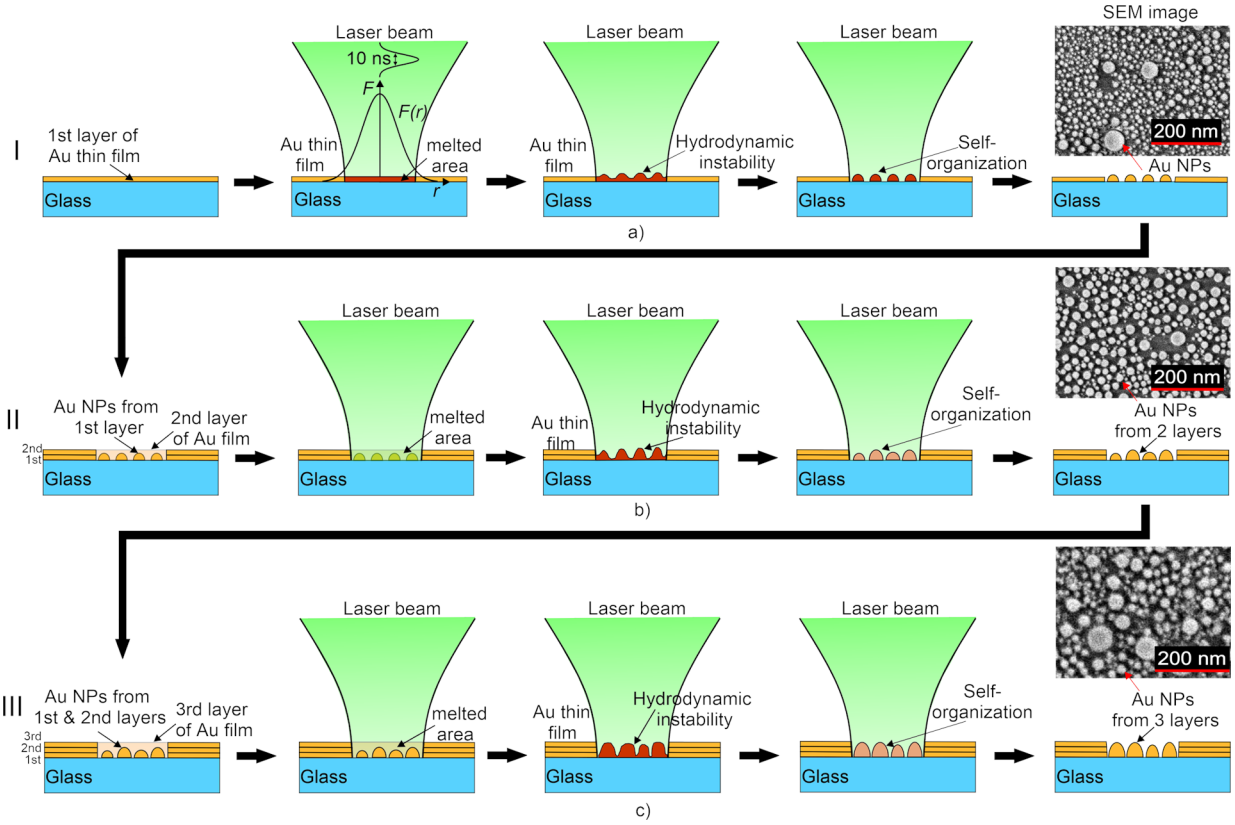

Figure 1. Generation of AuNPs on a glass substrate using single (a), double (b), and triple (c) layers of the gold film treatment with a nanosecond laser.

and template creation. The fabrication process primarily is based on a spinodal dewetting process in the melted gold film.[40] Due to the repeated processes of deposition and laser treatment, the fabricated SERS substrates have a higher enhancement of the Raman signal than the substrates manufactured from a single layer of the gold film. The Raman signal enhancement is related to the gaps between the nanoparticles, otherwise known as the "hot spots". The SERS substrates fabricated from the multilayer films have a higher density of nanoparticles; therefore, the density of the "hot spots" is higher. By coating the thin film of gold (5 nm), the density of "hot spots" in the substrate fabricated using a single layer of gold is increased, and the enhancement of the Raman signal also increases significantly. For the substrates fabricated using multilayer films, the coating of the thin gold film reduces the signal enhancement. It can be related to the smoothing of the surface by the coating.

The suggested fabrication approach of the SERS substrate is simple, reliable, and cost-effective compared to lithographical methods.[41,42] The main advantages of the nanosecond laser treatment are the short processing time, simple sample preparation process, submicron treatment accuracy, repeatability of samples, the low thermal impact to the substrate and surrounding areas, and the selective generation of nanoparticles at the desired place and of the desired shape at the surface.[43,44] The estimated EF of the fabricated SERS substrates is 10^6, similar to the conventional SERS EF.[45]

2. MATERIALS AND METHODS

2.1. Preparation of Gold Films on Glass. Gold films were prepared on a soda-lime glass substrate using magnetron sputtering at room temperature in an Ar atmosphere of 10^{-3} bar with a deposition rate of 0.2 nm/s (Quorum Q150T). The film thickness of gold films was controlled by varying the sputtering time from 25 to 50 s. This corresponds to 5 and 10 nm gold film thicknesses, respectively. Before the deposition, the glass substrates were cleaned with isopropanol and dried at room temperature.

2.2. Laser System for the Generation of Gold Nanoparticles. Gold nanoparticle (AuNP) generation from the prepared thin films on a glass substrate was realized in the air at room temperature by employing the nanosecond laser Ekspla Baltic operating at 532 nm wavelength with 75 mW average power, 10 ns pulse duration, and 500 Hz repetition rate. The diameter of the Gaussian beam on the surface was ~30 μm (at the level of $1/e^2$). The hatch (the distance between laser scanning lines) was selected to be 25 μm, and the beam scanning speed was 25 mm/s. In the experiments, two different thicknesses of the gold film on glass (5 and 10 nm) were used for the generation of AuNPs. The thicknesses of the coating were selected to be 5 and 10 nm according to the previous experiments.[40] The generation of AuNPs from the films thicker than 10 nm leads to a low concentration of AuNPs on a glass substrate.

2.3. Characterization of the Samples. *Scanning Electron Microscopy Characterization.* The samples were characterized using a scanning electron microscope Helios NanoLab650. All samples were imaged directly without the additional coating. The identification and the size measurements of the generated AuNPs were performed by processing scanning electron microscopy (SEM) images with the ImageJ program.

https://doi.org/10.1021/acsomega.1c05165
ACS Omega 2021, 6, 33889−33898

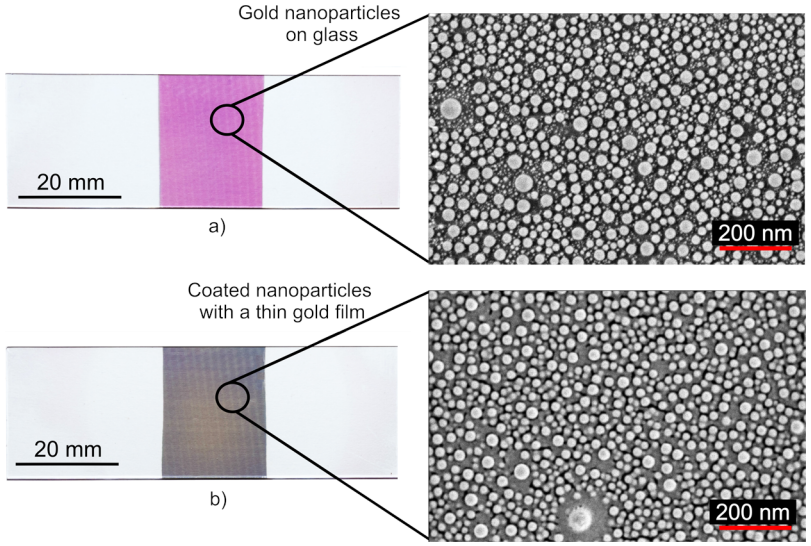

Figure 2. Examples of fabricated SERS substrates containing AuNPs generated from a triple layer of the 10 nm gold film (a) and coated with the 5 nm gold film (b). The size of the active area is ~25 × 20 mm^2.

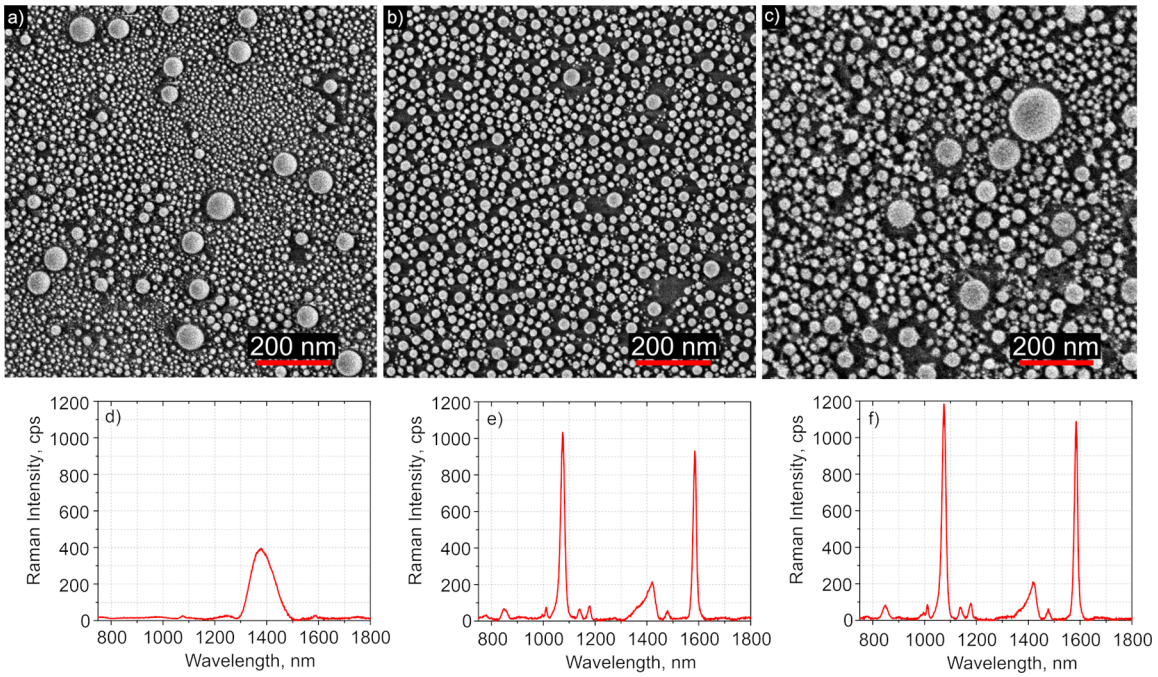

Figure 3. SEM micrographs of AuNPs generated on a glass substrate using a laser treatment of single (a), double (b), and triple (c) layers of 5 nm gold films and Raman spectra of 4-MBA by using AuNPs generated from single (d), double (e), and triple (f) layers of the 5 nm thick gold film. The nanoparticles were generated using 75 mW average laser power, 500 Hz repetition rate, 25 mm/s laser scanning speed, and a 25 μm hatch.

Optical Properties Measurements. Optical properties measurements were carried out using a spectrophotometer EssentOptics Photon RT. The transmission and reflectance spectra of the substrates were obtained within the wavelength range from 400 to 900 nm. The incidence angle in the measurements of the reflectance and transmission spectra was 8°. The used light beam spot size during the experiments was 2 × 5 mm^2.

Raman Measurements. Raman spectra were measured using an inVia (Renishaw) Raman spectrometer. The excitation source was a diode laser operating at a 785 nm wavelength with 0.9 mW average power and a thermoelectrically cooled (−70 °C) charge-coupled device camera. Using a 50×/0.50 NA long working distance objective, the laser beam was focused to a 1.8 μm diameter spot onto the investigated surface. 1200 lines/mm grating was used to record the Raman spectra. The accumulation time was 100 s. The Raman wavenumber axis was calibrated by the Si−Si vibrational mode at 520.7 cm^{-1}.

Samples Preparation for the Raman Measurements. The samples were immersed in a 1 mM solution of 4-mercaptobenzoic acid (4-MBA) (Figure S1) in ethanol for 16 h. Before the measurements, the samples were rinsed with ethanol (96%) and dried at room temperature after the purge with nitrogen gas.

https://doi.org/10.1021/acsomega.1c05165
ACS Omega 2021, 6, 33889−33898

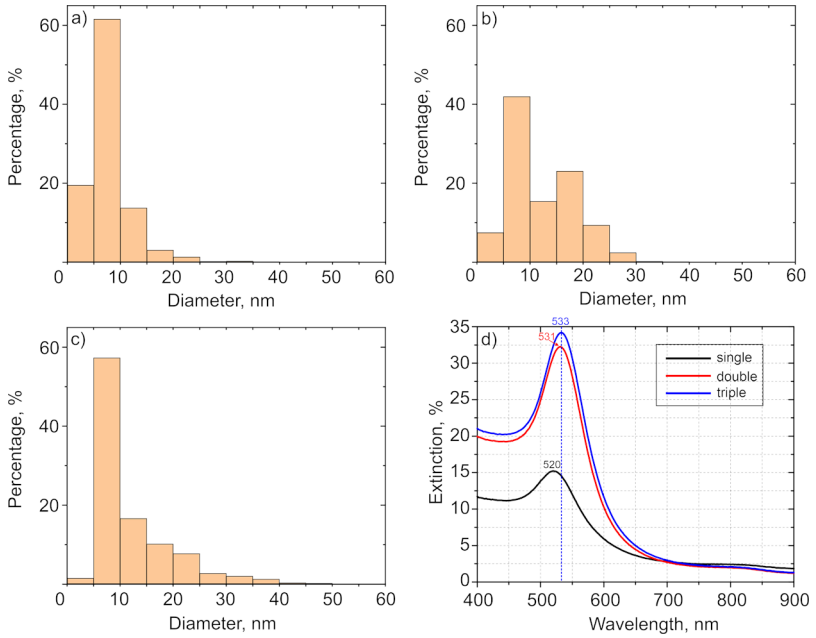

Figure 4. Size distribution (a−c) and extinction spectra (d) of AuNPs generated from single (a), double (b), and triple (c) layers of the 5 nm thick gold films. Bin size in all histograms is 5 nm. The estimation of the AuNP size distribution was taken from the 1040 × 700 nm^2 area. The blue dot line in (d) shows the maximum value of the extinction spectra of AuNPs generated from the triple gold layer.

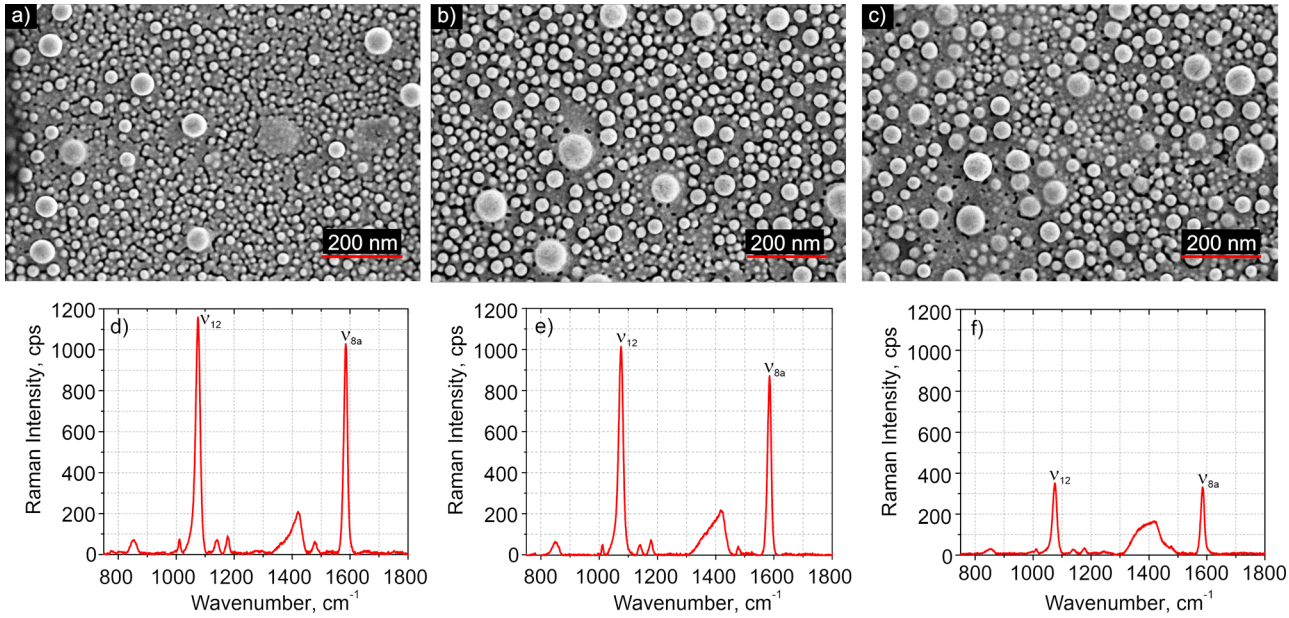

Figure 5. SEM micrographs of AuNPs generated on a glass substrate using the laser treatment of single (a), double (b), and triple (c) layers of 5 nm gold films with an additionally coated 5 nm gold film on the top and Raman spectra of 4-MBA by using AuNPs generated from single (d), double (e), and triple (f) layers of 5 nm thick gold films with an additionally coated 5 nm gold film on the top. The nanoparticles were generated using 75 mW average laser power, 500 Hz repetition rate, 25 mm/s laser scanning speed, and a 25 μm hatch.

Estimation of the EF of SERS Substrates. The EF was evaluated using the following equation:[7,46] EF = $(I_{SERS} \times N_R)/(I_R \times N_{SERS})$, where EF is the enhancement factor; I_{SERS} is the measured SERS integrated intensity of the monolayer substrate; I_R is the measured integrated intensity of the nonenhanced or normal Raman scattering from a bulk sample; N_{SERS} is the number of molecules under laser illumination at the surface, and N_R is the number of molecules under laser illumination in a bulk compound solution. For nonenhanced Raman scattering was used a 1 mm thickness quartz cell filled with 0.25 M 4-MBA ethanol solution. The AuNP substrates covered with a self-assembled monolayer of 4-MBA were used in SERS measurements. The most intensive vibrational modes of adsorbed 4-MBA at 1074 and 1584 cm^{-1} were used to determine the EF.

3. RESULTS AND DISCUSSION

3.1. Generation of AuNPs on a Glass Substrate. The generation of AuNPs on a glass substrate from multilayer thin gold films by using the nanosecond laser irradiation is

https://doi.org/10.1021/acsomega.1c05165
ACS Omega 2021, 6, 33889−33898

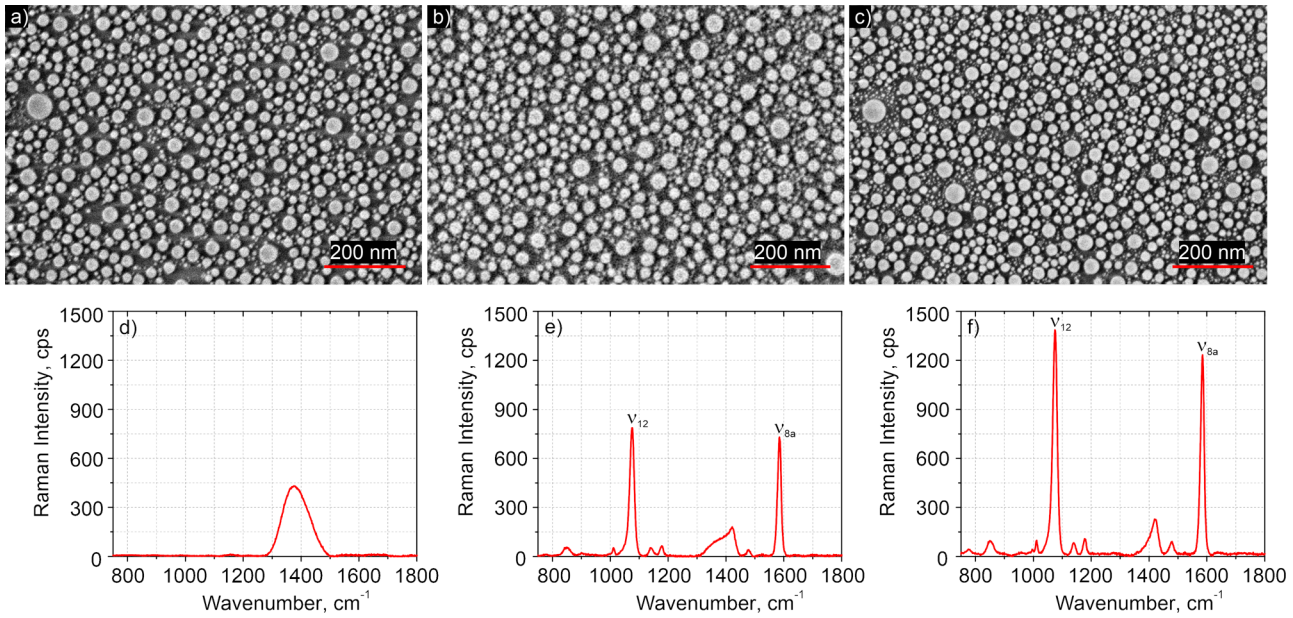

Figure 6. SEM micrographs of AuNPs generated on a glass substrate using a laser treatment of single (a), double (b), and triple (c) layers of 10 nm gold films and Raman spectra of 4-MBA by using AuNPs generated from single (d), double (e), and triple (f) layers of 10 nm thick gold films. The nanoparticles were generated using 75 mW average laser power, 500 Hz repetition rate, 25 mm/s laser scanning speed, and a 25 μm hatch.

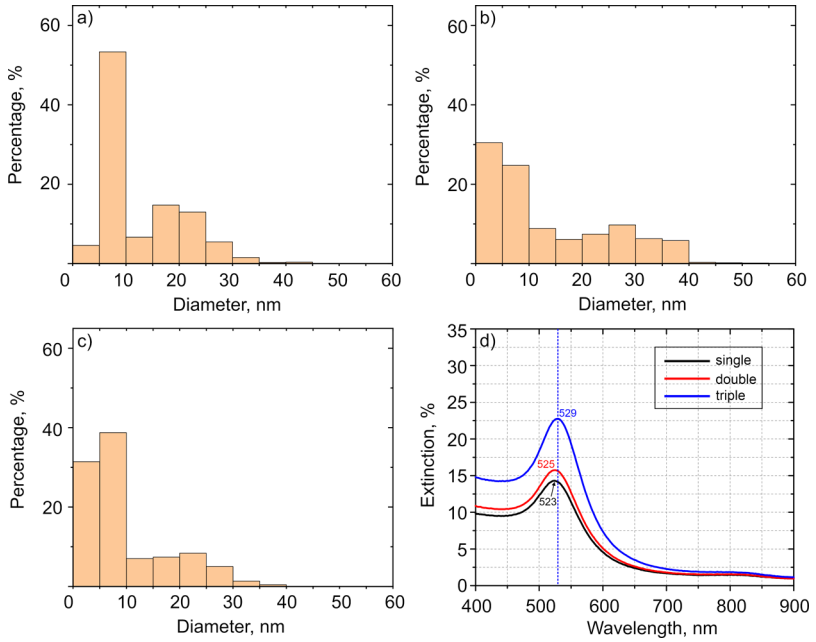

Figure 7. Size distribution (a−c) and extinction spectra (d) of AuNPs generated from single (a), double (b), and triple (c) layers of 10 nm thick gold films. Bin size in all histograms is 5 nm. The estimation of the AuNP size distribution was taken from the 1040 × 700 nm^2 area. The blue dot line in (d) shows the maximum value of the extinction spectra of AuNPs generated from the triple gold layer.

schematically illustrated in Figure 1. The generation of AuNPs was performed using single, double, and triple layers of gold films. At first, a thin (5 or 10 nm) gold layer deposited on a glass substrate is irradiated by the nanosecond laser beam (Figure 1a). During the nanosecond laser irradiation, the thin gold layer melts and stays in the molten phase as the energy transfer from the electron subsystem to the lattice is slow in gold.[47] In this case, the equilibrium between the hot electrons and lattice takes place within a time limit of up 50 ps.[48,49] In the melted thin gold film, hydrodynamic instabilities occur, causing self-organization of the material to the droplets on the glass. When the droplets cool down, they form AuNPs from a single layer of the gold film. Then, the generated nanoparticles are coated by the second layer of the thin (5 or 10 nm) gold film and processed with a laser, resulting in the fabrication of AuNPs from a double layer of the gold film (Figure 1b). AuNPs from a triple layer of the gold film are prepared by coating the thin film gold layer on the AuNPs generated from the double layer and treating it with the laser (Figure 1c). The formation of AuNPs using the nanosecond laser irradiation of the thin metallic coatings can be explained merely by the spinodal dewetting process.[50−52] The spinodal dewetting in the

https://doi.org/10.1021/acsomega.1c05165
ACS Omega 2021, 6, 33889−33898

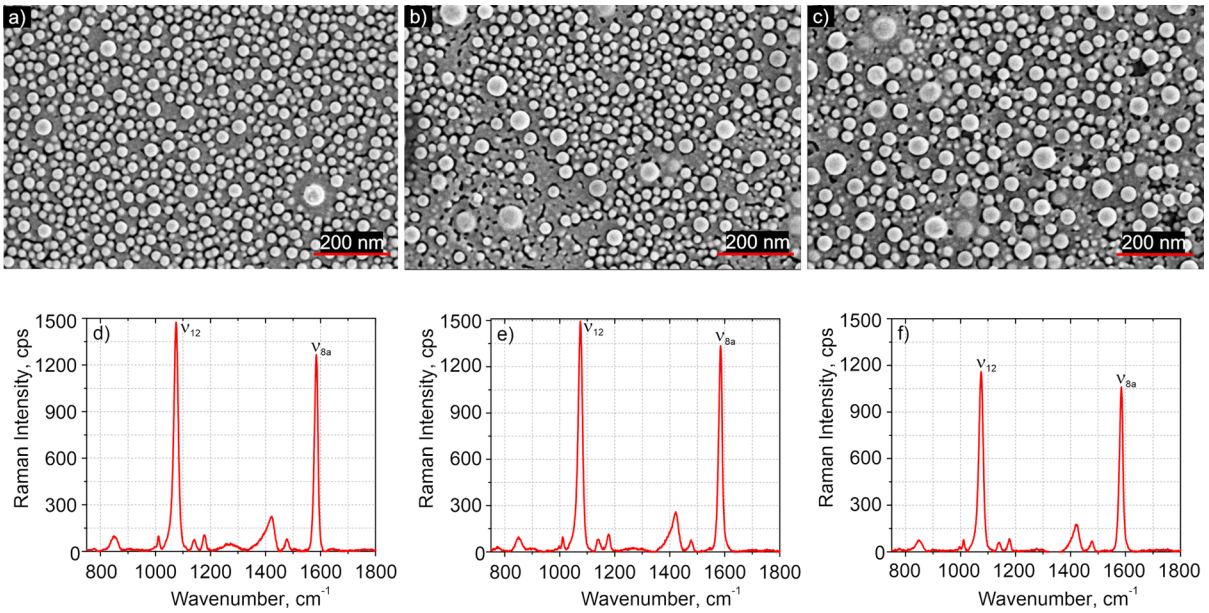

Figure 8. SEM micrographs of AuNPs generated on a glass substrate using a laser treatment of single (a), double (b), and triple (c) layers of 10 nm gold films with an additionally coated 5 nm gold film on the top and Raman spectra of 4-MBA by using AuNPs generated from single (d), double (e), and triple (f) layers of 10 nm thick gold films with an additionally coated 5 nm gold film on the top. The nanoparticles were generated using 75 mW average laser power, 500 Hz repetition rate, 25 mm/s laser scanning speed, and a 25 μm hatch.

Table 1. Evaluated EF for Each AuNP Substrate

substrate	EF for the ν_{12} mode (1074 cm^{-1})	EF for the ν_{8a} mode (1584 cm^{-1})
one layer from the 5 nm Au film without the coating	2.30×10^4	1.59×10^4
two layers from the 5 nm Au film without the coating	1.95×10^6	1.32×10^6
three layers from the 5 nm Au film without the coating	2.16×10^6	1.52×10^6
one layer from the 5 nm Au film with a 5 nm coating of gold	2.16×10^6	1.45×10^6
two layers from the 5 nm Au film with a 5 nm coating of gold	1.91×10^6	1.32×10^6
three layers from the 5 nm Au film with a 5 nm coating of gold	6.29×10^5	4.51×10^5
one layer from the 10 nm Au film without the coating	none	none
two layers from the 10 nm Au film without the coating	1.49×10^6	1.01×10^6
three layers from the 10 nm Au film without the coating	2.57×10^6	1.68×10^6
one layer from the 10 nm Au film with a 5 nm coating of gold	2.85×10^6	1.80×10^6
two layers from the 10 nm Au film with a 5 nm coating of gold	2.80×10^6	1.91×10^6
three layers from the 10 nm Au film with a 5 nm coating of gold	2.19×10^6	1.50×10^6

melted thin film occurs when attractive intermolecular forces exceed the stabilizing effect of the interfacial tension.[53,54] Then, the thin film becomes unstable, and the thermal fluctuations start to grow. The growth of the thermal fluctuations leads to the spontaneous destabilization of the thin film and the formation of droplets/nanoparticles.[55]

3.2. Characterization of AuNPs Prepared from 5 nm Films. The example of a glass substrate coated with AuNPs using the laser-based technique is shown in Figure 2a. Figure 2b shows a substrate with AuNPs coated with a 5 nm gold film. The uncoated substrate has a pink color, which is determined by LSPR.

The SEM images of AuNPs generated from single, double, and triple layers of 5 nm thick gold films are shown in Figure 3a,b. The size distribution of AuNPs for this case is presented in Figure 4a−c, which was estimated from a 1040 × 700 nm^2 area using the analysis of the SEM images with ImageJ software.[40] The total number of nanoparticles taken in each sample analysis is more than 1000. The nanoparticle size histogram shows that by increasing the number of gold film layers, the quantity of nanoparticles larger than 20 nm is increased. Moreover, in all cases, a large number of small nanoparticles (5−20 nm) is observed. The nanoparticles larger than 50 nm make up less than 1% of all nanoparticles. The optical spectra of generated nanoparticles show that the extinction is enhanced by increasing the number of coating layers (Figure 4d). This indicates that the density of the AuNPs is higher for a larger number of layers. Furthermore, the extinction spectra of the nanoparticles generated from double and triple layers have a small red shift compared to nanoparticles formed from a single layer. The red shift of the spectra (from 520 nm to 533 nm) indicates the increase in the size of nanoparticles.

The measured Raman spectra of 4-MBA by using AuNPs generated from single, double, and triple layers of the 5 nm thick gold film on a glass substrate are shown in Figure 3d−f. The spectra indicate that the AuNPs generated from a single layer of the 5 nm thick gold film exhibit very weak enhancement of the Raman scattering (Figure 3d). The broad feature near 1380 cm^{-1} is related to the glass substrate. When AuNPs are generated from double and triple gold layers, the intensity of the Raman signal of 4-MBA increases (Figure 3e,f). Two dominant bands in the SERS spectra near 1074 and 1589 cm^{-1} are related to the ring breathing + symmetric C−H in-plane bending + C−S stretching (the ν_{12} mode according to the Wilson notation for the description of ring vibrations) and ring C═C stretching + asymmetric C−H in-plane bending

https://doi.org/10.1021/acsomega.1c05165
ACS Omega 2021, 6, 33889−33898

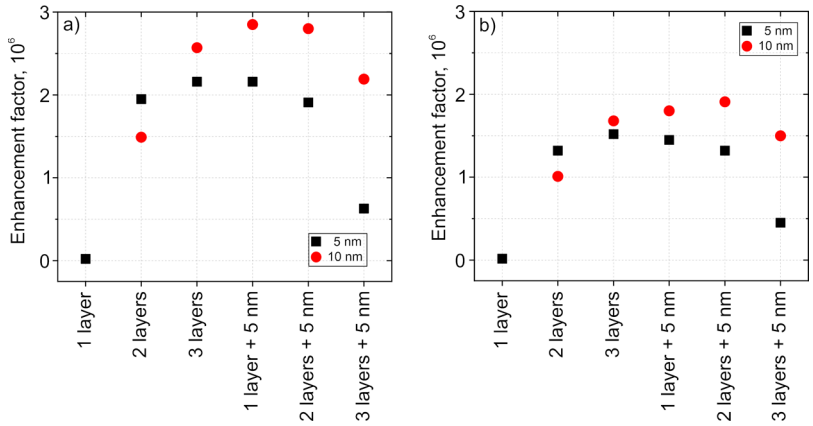

Figure 9. Estimated EFs for the ν_{12} mode (a) and ν_{8a} mode (b) of pure AuNPs (without a 5 nm gold coating on the top) generated from single, double, and triple layers of the gold film when the film thickness is 5 and 10 nm and the EF for the same AuNPs additionally coated with a 5 nm gold film on the top (noted "+ 5 nm" in the graphs).

(ν_{8a}) modes, respectively.[56,57] The broad band picked at 1420 cm^{-1} is due to the symmetric stretching vibration $\nu_s(COO^-)$ of the charged carboxylate group. A relatively high frequency value indicates that the carboxylate group remains unbound to the AuNPs.[56] Thus, the bonding of 4-MBA with the surface takes place primarily through the thiol moiety. The observed SERS spectra are clear and indicate the absence of bands from any impurities at the surface; all the bands are related to the vibrations of the adsorbed 4-MBA, except the broad feature near 1380 cm^{-1}, which is associated with the substrate.

The increase in the signal is related to the density of the nanoparticles. This can be followed by a corresponding increase in the extinction of the studied samples (Figure 4d). The higher extinction spectra indicate the higher density of nanoparticles. The higher density of the nanoparticles generated from double and triple layers have the higher amount of gaps between nanoparticles ("hot spots"). Therefore, the Raman signal of 4-MBA increases due to the enhancement in the electric field provided by the "hot spots". By adding the thin gold film (5 nm) on the top of the nanoparticles (Figure 5a−c), the Raman signal for the AuNPs generated from a single layer of the gold film is increased (Figure 5d), and this signal is higher than the Raman signal for AuNPs generated from double and triple layers of the gold film coated with the thin gold film (Figure 5e,f). When the density of AuNPs is lower, the coated thin gold film creates additional "hot spots" due to cracks in the coating (Figure 5a). When the density of AuNPs is higher (in double and triple layers), the coated thin gold film reduces the number of "hot spots" due to the smoothing of the gaps between AuNPs (Figure 5b,c). The roughness reduction of the created SERS substrate decreases the Raman signal (Figure 5e,f).[58] The larger the density of AuNPs on the substrate coated with a thin gold film is, the lower the enhancement of the Raman signal is.

3.3. Characterization of AuNPs Prepared from 10 nm Films. SEM images of the AuNPs generated using single, double, and triple layers of 10 nm gold films are presented in Figure 6a−c. By using 10 nm layers of gold films in the generation of AuNPs, a slight increase in the larger AuNPs (>20 nm) is observed compared to the use of 5 nm thick layers of gold films (Figure 7a−c). The red shift of the extinction spectra (from 523 to 529 nm) of nanoparticles (Figure 7d) indicates that the nanoparticles generated from a multilayer are slightly larger than the nanoparticles formed from a single 10 nm layer.

In this case, Raman spectra of 4-MBA for a single layer (Figure 6d) do not exhibit any enhancement of the Raman signal. The intensity in the Raman signal increases for AuNPs generated from double and triple layers of 10 nm gold films (Figure 6b,c) due to the higher density of AuNPs for a larger number of thin-film layers based on the optical spectra of generated nanoparticles from a different number of thin-film layers (Figure 7d). The Raman signal for the AuNPs generated from the triple layer of the 10 nm gold film is slightly higher compared to the Raman spectra for the AuNPs generated from the triple layer of the 5 nm gold film (Figure 6f). By adding a thin 5 nm gold film on the AuNPs, the Raman signal of 4-MBA for AuNPs generated from single and double 10 nm gold layers increases, while for a triple layer, it decreases compared to that of the AuNPs without the thin gold coating. The Raman signal enhancement tendency and reasons for the 10 nm gold film layer are very similar to that of the 5 nm gold film layers except that the signal is stronger due to the larger size of nanoparticles. Similar SERS spectra were observed at different places of the sample (Figure S2).

By adding a 5 nm gold coating on the nanoparticles generated from the multilayer of 10 nm films (SEM micrographs are shown in Figure 8a−c), the Raman signal in the single and double layer cases is increased significantly (Figure 8d,e) due to the emergence of the additional "hot spots" in the substrate, while the additional coating for the nanoparticles generated from a triple layer decreases the Raman signal (Figure 8f). The decrease in the Raman signal is related to the smoothing of the gaps between AuNPs.

3.4. Comparison of EFs. In the estimation of the EF of each substrate, the strongest vibrational modes for 4-MBA at 1074 and 1584 cm^{-1} were used. The gain of the vibrational mode ν_{12} (1074 cm^{-1}) is higher than that of the vibrational mode ν_{8a} (1584 cm^{-1}), probably because of the material interaction with the surface and orientational effects. The estimated EFs for each substrate for ν_{12} and ν_{8a} modes of 4-MBA are given in Table 1. The evaluated EF value for our studied AuNP substrates was similar to the conventional SERS EF (10^6).[45]

The summarization of the calculated EF for the SERS substrates consisting of the AuNPs generated from different numbers of 5 nm (black squares) and 10 nm (red circles) gold

https://doi.org/10.1021/acsomega.1c05165
ACS Omega 2021, 6, 33889−33898

films layers is given in Figure 9. The names "1, 2, and 3 layers" in the graphs mean the substrates consisting of the pure AuNPs generated from a single, double, or triple layer of gold films. The names "1, 2, and 3 layers + 5 nm" indicate that the SERS substrates are additionally coated with a 5 nm thin gold film. The EFs for both modes have the same tendency. The EF for SERS substrates coated with a 5 nm gold film is higher when the AuNPs are generated from the 10 nm gold films. For the uncoated AuNPs generated from 10 nm layers, the EF is higher only when the AuNPs are generated from the triple layer. When the substrates consist only of AuNPs generated from a single or double gold film layer, the EF is higher for AuNPs generated from 5 nm films (for a 10 nm single layer, the EF cannot even be estimated due to the low Raman signal enhancement). It can be related to the higher density of nanoparticles generated from the thinner films.

4. CONCLUSIONS

The fabrication of SERS substrates using a repeated process of a thin gold coating deposition and laser treatment of films is presented. The EF of the manufactured SERS substrates is similar to that of the conventional SERS substrates and is in a 10^6 value rank. The EF of the pure AuNPs generated from a single layer of the gold film can be significantly increased by adding a 5 nm gold coating on the top of the AuNPs. The additional coating on the AuNPs generated from the triple layer of gold films reduces the EF of the substrate due to the smoothing of the gaps between AuNPs. The demonstrated laser-based fabrication method of SERS substrates is simple, reliable, and cost-effective, which enables the large-scale fabrication of SERS substrates with high EFs at a low cost. Importantly, the proposed method produces a clean SERS substrate and does not require the use of chemicals for the reduction and stabilization of nanoparticles, thus avoiding the interference from the adsorbed impurities. Surface contamination is an important problem in the analysis of materials by using the SERS technique.[39]

ASSOCIATED CONTENT

Supporting Information

The Supporting Information is available free of charge at https://pubs.acs.org/doi/10.1021/acsomega.1c05165.

Molecular structure of 4-MBA, and SERS spectra at several places of the sample (PDF)

AUTHOR INFORMATION

Corresponding Author

Evaldas Stankevičius − *Department of Laser Technologies, Center for Physical Sciences and Technology (FTMC), LT-02300 Vilnius, Lithuania;* orcid.org/0000-0003-3783-5506; Email: evaldas.stankevicius@ftmc.lt

Authors

Ilja Ignatjev − *Department of Organic Chemistry, Center for Physical Sciences and Technology (FTMC), LT-10257 Vilnius, Lithuania*

Vita Petrikaitė − *Department of Laser Technologies, Center for Physical Sciences and Technology (FTMC), LT-02300 Vilnius, Lithuania*

Algirdas Selskis − *Department of Characterisation of Materials Structure, Center for Physical Sciences and Technology (FTMC), LT-10257 Vilnius, Lithuania*

Gediminas Niaura − *Department of Organic Chemistry, Center for Physical Sciences and Technology (FTMC), LT-10257 Vilnius, Lithuania*

Complete contact information is available at: https://pubs.acs.org/10.1021/acsomega.1c05165

Notes

The authors declare no competing financial interest.

ACKNOWLEDGMENTS

E.S, V.P., A.S., and G.N. acknowledge the funding from the European Regional Development Fund (project no. 01.2.2-LMT-K-718-03-0078) under a grant agreement with the Research Council of Lithuania (LMTLT).

REFERENCES

(1) Fleischmann, M.; Hendra, P. J.; McQuillan, A. J. Raman spectra of pyridine adsorbed at a silver electrode. *Chem. Phys. Lett.* **1974**, *26*, 163−166.

(2) Sharma, B.; Frontiera, R. R.; Henry, A.-I.; Ringe, E.; Van Duyne, R. P. SERS: Materials, applications, and the future. *Mater. Today* **2012**, *15*, 16−25.

(3) Schlücker, S. Surface-Enhanced Raman Spectroscopy: Concepts and Chemical Applications. *Angew. Chem., Int. Ed.* **2014**, *53*, 4756−4795.

(4) Starowicz, Z.; Wojnarowska-Nowak, R.; Ozga, P.; Sheregii, E. M. The tuning of the plasmon resonance of the metal nanoparticles in terms of the SERS effect. *Colloid Polym. Sci.* **2018**, *296*, 1029−1037.

(5) Zeng, Y.; Madsen, S. J.; Yankovich, A. B.; Olsson, E.; Sinclair, R. Comparative electron and photon excitation of localized surface plasmon resonance in lithographic gold arrays for enhanced Raman scattering. *Nanoscale* **2020**, *12*, 23768−23779.

(6) Álvarez-Puebla, R. A. Effects of the Excitation Wavelength on the SERS Spectrum. *J. Phys. Chem. Lett.* **2012**, *3*, 857−866.

(7) McFarland, A. D.; Young, M. A.; Dieringer, J. A.; Van Duyne, R. P. Wavelength-Scanned Surface-Enhanced Raman Excitation Spectroscopy. *J. Phys. Chem. B* **2005**, *109*, 11279−11285.

(8) Mayer, K. M.; Hafner, J. H. Localized Surface Plasmon Resonance Sensors. *Chem. Rev.* **2011**, *111*, 3828−3857.

(9) Bell, S. E. J.; Charron, G.; Cortés, E.; Kneipp, J.; Chapelle, M. L.; Langer, J.; Procházka, M.; Tran, V.; Schlücker, S. Towards Reliable and Quantitative Surface-Enhanced Raman Scattering (SERS): From Key Parameters to Good Analytical Practice. *Angew. Chem., Int. Ed.* **2020**, *59*, 5454−5462.

(10) Le Ru, E.; Etchegoin, P. *Principles of Surface-Enhanced Raman Spectroscopy and Related Plasmonic Effects*; Elsevier: Amsterdam, 2008; p 663.

(11) Le Ru, E. C.; Blackie, E.; Meyer, M.; Etchegoin, P. G. Surface Enhanced Raman Scattering Enhancement Factors:A Comprehensive Study. *J. Phys .Chem .C* **2007**, *111*, 13794−13803.

(12) Barbillon, G.; Bijeon, J.-L.; Plain, J.; de la Chapelle, M. L.; Adam, P.-M.; Royer, P. Electron beam lithography designed chemical nanosensors based on localized surface plasmon resonance. *Surf. Sci.* **2007**, *601*, 5057−5061.

(13) Yue, W.; Wang, Z.; Yang, Y.; Chen, L.; Syed, A.; Wong, K.; Wang, X. Electron-beam lithography of gold nanostructures for surface-enhanced Raman scattering. *J. Micromech. Microeng.* **2012**, *22*, 125007.

(14) Petti, L.; Capasso, R.; Rippa, M.; Pannico, M.; La Manna, P.; Peluso, G.; Calarco, A.; Bobeico, E.; Musto, P. A plasmonic nanostructure fabricated by electron beam lithography as a sensitive and highly homogeneous SERS substrate for bio-sensing applications. *Vib. Spectrosc.* **2016**, *82*, 22−30.

(15) Lin, Y.-Y.; Liao, J.-D.; Ju, Y.-H.; Chang, C.-W.; Shiau, A.-L. Focused ion beam-fabricated Au micro/nanostructures used as a surface enhanced Raman scattering-active substrate for trace detection of molecules and influenza virus. *Nanotechnology* **2011**, *22*, 185308.

(16) Sivashanmugan, K.; Liao, J.-D.; You, J.-W.; Wu, C.-L. Focused-ion-beam-fabricated Au/Ag multilayered nanorod array as SERS-active substrate for virus strain detection. *Sens. Actuators, B* **2013**, *181*, 361−367.
(17) Christou, K.; Knorr, I.; Ihlemann, J.; Wackerbarth, H.; Beushausen, V. Fabrication and Characterization of Homogeneous Surface-Enhanced Raman Scattering Substrates by Single Pulse UV-Laser Treatment of Gold and Silver Films. *Langmuir* **2010**, *26*, 18564−18569.
(18) Stankevičius, E.; Daugnoraitė, E.; Ignatjev, I.; Kuodis, Z.; Niaura, G.; Račiukaitis, G. Concentric microring structures containing gold nanoparticles for SERS-based applications. *Appl. Surf. Sci.* **2019**, *497*, 143752.
(19) Stankevičius, E.; Garliauskas, M.; Gedvilas, M.; Tarasenko, N.; Račiukaitis, G. Structuring of Surfaces with Gold Nanoparticles by Using Bessel-Like Beams. *Ann. Phys.* **2017**, *529*, 1700174.
(20) Jensen, T. R.; Malinsky, M. D.; Haynes, C. L.; Van Duyne, R. P. Nanosphere Lithography:Tunable Localized Surface Plasmon Resonance Spectra of Silver Nanoparticles. *J. Phys .Chem .B* **2000**, *104*, 10549−10556.
(21) Ormonde, A. D.; Hicks, E. C. M.; Castillo, J.; Van Duyne, R. P. Nanosphere Lithography:Fabrication of Large -AreaAg Nanoparticle Arrays by Convective Self -Assemblyand Their Characterization by Scanning UV−Visible Extinction Spectroscopy. *Langmuir* **2004**, *20*, 6927−6931.
(22) Zhao, X.; Wen, J.; Zhang, M.; Wang, D.; Wang, Y.; Chen, L.; Zhang, Y.; Yang, J.; Du, Y. Design of Hybrid Nanostructural Arrays to Manipulate SERS-Active Substrates by Nanosphere Lithography. *ACS Appl. Mater. Interfaces* **2017**, *9*, 7710−7716.
(23) Khan, M. A.; Hogan, T. P.; Shanker, B. Gold-coated zinc oxide nanowire-based substrate for surface-enhanced Raman spectroscopy. *J. Raman Spectrosc.* **2009**, *40*, 1539−1545.
(24) Cheng, C.; Yan, B.; Wong, S. M.; Li, X.; Zhou, W.; Yu, T.; Shen, Z.; Yu, H.; Fan, H. J. Fabrication and SERS Performance of Silver-Nanoparticle-Decorated Si/ZnO Nanotrees in Ordered Arrays. *ACS Appl. Mater. Interfaces* **2010**, *2*, 1824−1828.
(25) Li, Y.; Dykes, J.; Gilliam, T.; Chopra, N. A new heterostructured SERS substrate: free-standing silicon nanowires decorated with graphene-encapsulated gold nanoparticles. *Nanoscale* **2017**, *9*, 5263−5272.
(26) Liu, Y.; Fan, J.; Zhao, Y.-P.; Shanmukh, S.; Dluhy, R. A. Angle dependent surface enhanced Raman scattering obtained from a Ag nanorod array substrate. *Appl. Phys. Lett.* **2006**, *89*, 173134.
(27) Chaney, S. B.; Shanmukh, S.; Dluhy, R. A.; Zhao, Y.-P. Aligned silver nanorod arrays produce high sensitivity surface-enhanced Raman spectroscopy substrates. *Appl. Phys. Lett.* **2005**, *87*, 031908.
(28) Liu, Y.-J.; Chu, H. Y.; Zhao, Y.-P. Silver Nanorod Array Substrates Fabricated by Oblique Angle Deposition: Morphological, Optical, and SERS Characterizations. *J. Phys. Chem. C* **2010**, *114*, 8176−8183.
(29) Yang, Y.; Hu, Z.; Wang, Y.; Wang, B.; Zhan, Q.; Zhang, Y.; Ao, X. Broadband SERS substrates by oblique angle deposition method. *Opt. Mater. Express* **2016**, *6*, 2644−2654.
(30) Jana, N. R.; Pal, T. Anisotropic Metal Nanoparticles for Use as Surface-Enhanced Raman Substrates. *Adv. Mater.* **2007**, *19*, 1761−1765.
(31) Guo, Q.; Xu, M.; Yuan, Y.; Gu, R.; Yao, J. Self-Assembled Large-Scale Monolayer of Au Nanoparticles at the Air/Water Interface Used as a SERS Substrate. *Langmuir* **2016**, *32*, 4530−4537.
(32) Williamson, T. L.; Guo, X.; Zukoski, A.; Sood, A.; Díaz, D. J.; Bohn, P. W. Porous GaN as a Template to Produce Surface-Enhanced Raman Scattering-Active Surfaces. *J. Phys. Chem. B* **2005**, *109*, 20186−20191.
(33) Gao, P.; Gosztola, D.; Leung, L.-W. H.; Weaver, M. J. Surface-enhanced Raman scattering at gold electrodes: dependence on electrochemical pretreatment conditions and comparisons with silver. *J. Electroanal. Chem. Interfacial Electrochem.* **1987**, *233*, 211−222.
(34) Proniewicz, E.; Ignatjev, I.; Niaura, G.; Sobolewski, D.; Prahl, A.; Proniewicz, L. M. Role of Phe-D5 isotopically labeled analogues of bradykinin on elucidation of its adsorption mode on Ag, Au, and Cu electrodes. Surface-enhanced Raman spectroscopy studies. *J. Raman Spectrosc.* **2013**, *44*, 1096−1104.
(35) Sun, X.; Li, H. Gold nanoisland arrays by repeated deposition and post-deposition annealing for surface-enhanced Raman spectroscopy. *Nanotechnology* **2013**, *24*, 355706.
(36) Quan, J.; Zhang, J.; Qi, X.; Li, J.; Wang, N.; Zhu, Y. A study on the correlation between the dewetting temperature of Ag film and SERS intensity. *Sci. Rep.* **2017**, *7*, 14771.
(37) Barbillon, G.; Hamouda, F.; Held, S.; Gogol, P.; Bartenlian, B. Gold nanoparticles by soft UV nanoimprint lithography coupled to a lift-off process for plasmonic sensing of antibodies. *Microelectron. Eng.* **2010**, *87*, 1001−1004.
(38) Suresh, V.; Ding, L.; Chew, A. B.; Yap, F. L. Fabrication of Large-Area Flexible SERS Substrates by Nanoimprint Lithography. *ACS Appl. Nano Mater.* **2018**, *1*, 886−893.
(39) Lin, X.-M.; Cui, Y.; Xu, Y.-H.; Ren, B.; Tian, Z.-Q. Surface-enhanced Raman spectroscopy: substrate-related issues. *Anal. Bioanal. Chem.* **2009**, *394*, 1729−1745.
(40) Stankevičius, E.; Garliauskas, M.; Laurinavičius, L.; Trusovas, R.; Tarasenko, N.; Pauliukaitė, R. Engineering electrochemical sensors using nanosecond laser treatment of thin gold film on ITO glass. *Electrochim. Acta* **2019**, *297*, 511−522.
(41) Green, M.; Liu, F. M. SERS Substrates Fabricated by Island Lithography:The Silver /PyridineSystem. *J. Phys .Chem .B* **2003**, *107*, 13015−13021.
(42) Cottat, M.; Lidgi-Guigui, N.; Tijunelyte, I.; Barbillon, G.; Hamouda, F.; Gogol, P.; Aassime, A.; Lourtioz, J.-M.; Bartenlian, B.; de la Chapelle, M. L. Soft UV nanoimprint lithography-designed highly sensitive substrates for SERS detection. *Nanoscale Res. Lett.* **2014**, *9*, 623.
(43) Lin, Y.; Zhai, T.; Zhang, X. Nanoscale heat transfer in direct nanopatterning into gold films by a nanosecond laser pulse. *Opt. Express* **2014**, *22*, 8396−8404.
(44) Pang, Z.; Zhang, X. Direct writing of large-area plasmonic photonic crystals using single-shot interference ablation. *Nanotechnology* **2011**, *22*, 145303.
(45) Cinel, N. A.; Çakmakyapan, S.; Ertas, G.; Özbay, E. Concentric Ring Structures as Efficient SERS Substrates. *IEEE J. Sel. Top. Quantum Electron.* **2013**, *19*, 4601605.
(46) Yu, H.-Z.; Zhang, J.; Zhang, H.-L.; Liu, Z.-F. Surface-Enhanced Raman Scattering (SERS) from Azobenzene Self-Assembled "Sandwiches". *Langmuir* **1999**, *15*, 16−19.
(47) Unger, C.; Koch, J.; Overmeyer, L.; Chichkov, B. N. Time-resolved studies of femtosecond-laser induced melt dynamics. *Opt. Express* **2012**, *20*, 24864−24872.
(48) Ivanov, D. S.; Zhigilei, L. V. Combined atomistic-continuum modeling of short-pulse laser melting and disintegration of metal films. *Phys. Rev. B: Condens. Matter Mater. Phys.* **2003**, *68*, 064114.
(49) Ruffino, F.; Pugliara, A.; Carria, E.; Romano, L.; Bongiorno, C.; Fisicaro, G.; La Magna, A.; Spinella, C.; Grimaldi, M. G. Towards a laser fluence dependent nanostructuring of thin Au films on Si by nanosecond laser irradiation. *Appl. Surf. Sci.* **2012**, *258*, 9128−9137.
(50) Trice, J.; Thomas, D.; Favazza, C.; Sureshkumar, R.; Kalyanaraman, R. Pulsed-laser-induced dewetting in nanoscopic metal films: Theory and experiments. *Phys. Rev. B: Condens. Matter Mater. Phys.* **2007**, *75*, 235439.
(51) Herminghaus, S.; Jacobs, K.; Mecke, K.; Bischof, J.; Fery, A.; Ibn-Elhaj, M.; Schlagowski, S. Spinodal Dewetting in Liquid Crystal and Liquid Metal Films. *Science* **1998**, *282*, 916−919.
(52) Favazza, C.; Kalyanaraman, R.; Sureshkumar, R. Robust nanopatterning by laser-induced dewetting of metal nanofilms. *Nanotechnology* **2006**, *17*, 4229.
(53) Sharma, A.; Ruckenstein, E. Finite-amplitude instability of thin free and wetting films: prediction of lifetimes. *Langmuir* **1986**, *2*, 480−494.
(54) Seemann, R.; Herminghaus, S.; Jacobs, K. Dewetting Patterns and Molecular Forces: A Reconciliation. *Phys. Rev. Lett.* **2001**, *86*, 5534−5537.

https://doi.org/10.1021/acsomega.1c05165
ACS Omega 2021, 6, 33889−33898

(55) Bonn, D.; Eggers, J.; Indekeu, J.; Meunier, J.; Rolley, E. Wetting and spreading. *Rev. Mod. Phys.* **2009**, *81*, 739−805.
(56) Ho, C.-H.; Lee, S. SERS and DFT investigation of the adsorption behavior of 4-mercaptobenzoic acid on silver colloids. *Colloids Surf., A* **2015**, *474*, 29−35.
(57) Michota, A.; Bukowska, J. Surface-enhanced Raman scattering (SERS) of 4-mercaptobenzoic acid on silver and gold substrates. *J. Raman Spectrosc.* **2003**, *34*, 21−25.
(58) Rodríguez-Fernández, J.; Funston, A. M.; Pérez-Juste, J.; Álvarez-Puebla, R. A.; Liz-Marzán, L. M.; Mulvaney, P. The effect of surface roughness on the plasmonic response of individual sub-micron gold spheres. *Phys. Chem. Chem. Phys.* **2009**, *11*, 5909−5914.

https://doi.org/10.1021/acsomega.1c05165
ACS Omega 2021, 6, 33889−33898